Chinese Journal of
POLYMER SCIENCE

RESEARCH ARTICLE

https://doi.org/10.1007/s10118-026-3736-0
Chinese J. Polym. Sci.

Molecular Dynamics Investigation of the Mechanism of Poly(vinyl chloride) Plasticization by Dicarboxylic Acid Esters

Gennady I. Makarov[a*], Irina N. Vikhareva[a], and Oleg I. Bol'shakov[b,c]

[a] *South Ural State University, 76, Lenin prospekt, Chelyabinsk 454080, Russia*
[b] *Nanotechnology Education and Research Center, South Ural State University, 76, Lenin prospekt, Chelyabinsk 454080, Russia*
[c] *Laboratory of Cell Hemostasis, National Medical Research Centre of Cardiology named after Academician E.I. Chazov of the Ministry of Health of the Russian Federation, 15A, Akademika Chazova st., Moscow 121552, Russia*

Electronic Supplementary Information

Abstract Polymer compositions based on plasticized poly(vinyl chloride) (PVC) are extremely widely used in engineering and everyday life. Diester plasticizers based on aliphatic dicarboxylic acids are currently considered as new, environmentally friendly, and less toxic plasticizers for poly(vinyl chloride). In the present work, the structural organization of polymer compositions based on poly(vinyl chloride) plasticized with dicarboxylic acid diesters—dibutoxyethyl glutarate, dibutoxyethyl adipate, octyl butoxyethyl adipate, dibutoxyethyl azelate, and dibutoxyethyl sebacate—was studied using molecular dynamics modeling methods. The methodology of fragment condensation was used to obtain three-dimensional models of the dense polymer phase. It is shown that the intensity of intermolecular interactions between PVC chains and plasticizer molecules, as well as the degree of uniformity of the plasticizer's spatial distribution, directly affect the characteristics of the temperature dependence of the mechanical loss tangent. Thereby, the heterogeneity of the plasticizer distribution at the nanoscale level, determined by its tendency to associate, significantly affects the width of the glass transition. The data suggest a possible transition from a plasticization mechanism characteristic of short-chain diesters (associated with a higher number of directional Cl···O contacts) to a mechanism of bulk dispersion spacing of PVC chains for long-chain esters. This interpretation is consistent with the observed differences in thermal stability and low-temperature flexibility. These conclusions are based on a limited set of five plasticizers and a specific MD/fragment-condensation framework; therefore, they should be considered as preliminary and model-dependent.

Keywords Molecular dynamics; Poly(vinyl chloride); Plasticizer; Ester; Halogen bonds; Microinhomogeneity; Relaxation behavior

Citation: Makarov, G. I.; Vikhareva, I. N.; Bol'shakov, O. I. Molecular dynamics investigation of the mechanism of poly(vinyl chloride) plasticization by dicarboxylic acid esters. *Chinese J. Polym. Sci.* https://doi.org/10.1007/s10118-026-3736-0

INTRODUCTION

Poly(vinyl chloride) (PVC) holds one of the leading positions in the world of polymeric materials in terms of production and consumption volumes, being second only to polyolefins.[1] This popularity is caused by a unique combination of performance characteristics: high chemical resistance, strength, durability, dielectric properties, and relatively low cost.[2] Therefore, PVC finds extremely wide application in construction (window profiles, pipes, floor coverings), medicine (containers, tubes), packaging production, cable insulation, and many other fields.[3] However, "pure" PVC is a rigid and brittle material with a limited processing temperature range. Overcoming these shortcomings and imparting the required properties to the material, such as flexibility, elasticity, frost resistance, and processability, is the main task in creating practical compositions.

Plasticizers, playing a fundamental role in solving this problem, are substances introduced into the polymer matrix to increase its flexibility and elasticity by reducing the intermolecular interactions of the PVC chains.[4] The type and amount of plasticizer determine the purpose and application area of the final product, as well as its main characteristics. Thus, the diversity of PVC-based materials is directly related to the wide range of available plasticizers and their effectiveness. For a long time, this niche was almost monopolistically occupied by phthalate plasticizers, particularly di(2-ethylhexyl) phthalate (DOP), owing to their high efficiency and low cost.[5]

In recent decades, attention to the toxicological and environmental aspects of using traditional plasticizers has increased. A number of phthalates, including DOP, have been subject to strict regulation due to their potential disruptive effects on the endocrine system and their ability to bioaccumulate.[6] This has stimulated an active search for alternative, safer compounds as potential plasticizers. Diester plasticizers based on aliphatic dicarboxylic acids (*e.g.*, sebacic and adipic acids) are among the most promising alternatives.[7]

* Corresponding author, E-mail: makarovgi@susu.ru
Received March 17, 2026; Accepted May 5, 2026; Published online July 24, 2026

These compounds demonstrate plasticizing efficiency comparable to that of phthalates, but possess improved environmental and toxicological profiles and often provide better low-temperature flexibility.[8]

The optimization of the formulation of a PVC composition for specific tasks is a complex multi-parameter problem. The empirical selection of the plasticizer and its concentration is time-consuming and expensive. To rationalize it, an understanding of the fundamental relationships between the molecular structure of the plasticizer, the features of its interaction with the polymer, the structural organization of the resulting mixture, and the physicochemical properties of the material is necessary.[9,10] The key nexus in this chain is the structure of the plasticized polymer phase. Since PVC compositions are amorphous systems, the capabilities of their investigation by experimental methods, such as X-ray diffraction analysis, are limited.[11] Methods that enable to estimate assessing chain movability, such as dynamic mechanical analysis or NMR relaxation, provide an integral image, but do not reveal the details of the structural organization at the atomic-molecular level, such as the spatial distribution of plasticizer molecules, local density, nature of hydrogen bonds, and van der Waals interactions.

In this context, the method of molecular dynamics (MD) modelling becomes a powerful tool that enables to model the structure of polymer materials and to calculate the physicochemical properties determined by it. For example, MD modelling makes it possible to calculate the dielectric constant for polyolefins[12] and successfully reproduces the experimentally measured diffusion coefficients for hydrogenated polybutadiene.[13] Using this method, the permeability of PVC membranes for hydrocarbons was investigated.[14] MD modelling was applied to model the structure and properties of plasticized PVC compositions; for example, to model the structure and properties of poly(vinyl chloride) plasticized with dioctyl phthalate[15], successfully reproducing the solubility parameter, or to study the plasticizing action of a mixture of isosorbide diheptanoate and dioctyl phthalate on PVC.[16] Thus, the MD method has been successfully used to study materials based on poly(vinyl chloride), acting as a powerful method for establishing relationships between the structural organization of a polymer material and its macroscopically observed properties.

Recent computational studies have significantly advanced our understanding of PVC plasticization. For instance, Li *et al.*[17] performed atomistic simulations to systematically evaluate the compatibility and efficacy of phthalate plasticizers, demonstrating that alkyl side-chain relaxation is the limiting step for plasticizer migration. In a comprehensive follow-up study, Li *et al.*[18] established a framework of seven molecular design parameters that govern the plasticizer performance, including compatibility, modulus reduction, and migration rate. Separately, Zhou and Milner[19] investigated concentration-dependent glass transition temperature (T_g) shifts in PVC/DEHP blends, revealing an exponential decay of local T_g reduction with distance from the plasticizer molecules. While these studies have provided invaluable insights, they have primarily focused on phthalate-based plasticizers and their blends with PVC. Our study extends this knowledge to a new class of environmentally friendly dicarboxylic acid esters and, crucially, links the molecular-level insights from MD simulations with a comprehensive set of experimentally measured macroscopic properties—such as rheological behavior, dynamic mechanical relaxation, and thermal stability—to establish robust structure–property relationships.

In the present work we studied the structural organization of polymer compositions based on poly(vinyl chloride) plasticized with dicarboxylic acid esters. The aim of our study was to construct structural models of the polymer phases formed by PVC molecules with a number-average molecular weight of 91 kDa and plasticizers—esters of glutaric, adipic, azelaic, and sebacic acids—in order to establish the relationship between the molecular structure of the plasticizers and the main physicochemical properties of the polymer compositions based on them.

METHODS

Methods of MD Simulations

Molecular mechanical models of poly(vinyl chloride) residues, dicarboxylic acid esters, and bisphenol A were prepared using the General Amber force field (GAFF).[20] Partial charges were obtained using the RESP[21] model. The optimized three-dimensional structures of parameterized residues and their molecular electrostatic potentials were calculated using the M062X/6–311++G(d,p) density functional theory method in ORCA 5.0.3 package.[22,23]

Calculations and analysis of MD trajectories were performed using GROMACS[24] 2019.4 software. Coordinates were written to the trajectory file every 5000 simulation steps, and the integration step of the equations of motion was 2 fs, unless otherwise stated. The temperature was maintained by the velocity rescaling thermostat with additional stochastic correction.[25] The constant anisotropic pressure was maintained by the Berendsen barostat[26] with a coupling time of 5 ps. Bond lengths were constrained using the LINCS[27] algorithm. The Ewald particle mesh method with a 0.1 nm grid step and the sixth order interpolation was used to handle long–range electrostatic[28] and van der Waals[29] interactions.

Modelling of Dense PVC Compositions

Poly(vinyl chloride) (PVC) compositions plasticized with dibutoxyethyl glutarate, dibutoxyethyl adipate (DBEA), octyl butoxyethyl adipate (OBEA), dibutoxyethyl azelate (DBEAz), and dibutoxyethyl sebacate (DBES) (Fig. 1) were selected for modelling. This selection of modelled polymer compositions comprises all classes of plasticizers with respect to acid residues and the symmetry/asymmetry of the ester substituents. Composition of the modelled compositions was set to match the composition of the experimentally studied samples: 100 weight parts of PVC S–7058M grade, 40 weight parts of plasticizer, and 0.25 weight parts of bisphenol A.[30,31] Bisphenol A is introduced into PVC compositions as an antioxidant additive, and it was present in the modelled systems only to reproduce the compositions of the experimentally studied PVC compositions.

To model the structure of the dense phase of plasticized PVC, we applied the fragment condensation methodology, which we previously developed and successfully applied it to model the ED–20 epoxy resin cured with triethylenete-

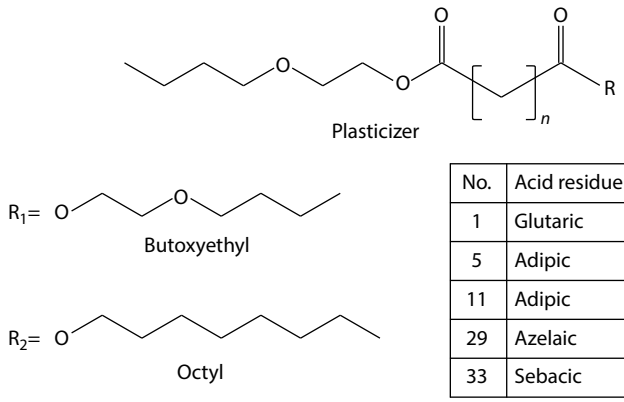

No.	Acid residue	*n*	R
1	Glutaric	3	R1
5	Adipic	4	R1
11	Adipic	4	R2
29	Azelaic	7	R1
33	Sebacic	8	R1

Fig. 1 Structures of diester plasticizers molecules studied in the present work. The *n* variable shows the number of methylene groups in the acid residue.

traamine[32] and the self-healing copolymer of *α,ω*-(aminopropyl)polydimethylsiloxane and 2,6-pyridinedicarbonyl dichloride cross-linked with nickel(II) ions.[33] The initial step of this approach is to construct a model of an equilibrated dense "liquid of residues" composed of short–chain fragments or individual residues of polymer chains and other components of the future polymer phase. Subsequently, the necessary crosslinks are introduced between the fragments of the polymer chains, which leads to the formation of densely packed polymer chains of the desired structure.

The "liquid of residues" was composed of molecules of diester plasticizers, bisphenol A, and short, six-membered poly(vinyl chloride) (PVC_6) chains upon modelling the selected PVC compositions. This size of the polymer fragments, on the one hand, ensured their easy movement within the simulation cell and high conformational flexibility due to the short polymer chain length. On the other hand, the length of their chains forced them to adopt conformations similar to those of short sections of long PVC chains. The exact compositions of the modelled compositions are given in Table 1.

Table 1 Compositions of modelled PVC compositions, molecules per simulation cell.

No.	Plasticizer type	PVC_6	Plasticizer	Bisphenol A
1	Dibutoxyethyl glutarate	487	220	2
5	Dibutoxyethyl adipate	487	210	2
11	Octyl butoxyethyl adipate	487	204	2
29	Dibutoxyethyl azelate	487	188	2
33	Dibutoxyethyl sebacate	487	176	2

The following operations were performed for each modelled composition. A "liquid of residues" was prepared in the first stage. Upon its preparation, all components of the modelled system were randomly placed in a cubic cell with an 18 nm edge. The potential energy of the constructed system was minimized using the flexible conjugate gradient method[34], after which a 5 ns MD simulation at a constant volume and a temperature of 2673 K was performed. Molecules of the modelled system were mixed and distributed throughout the cell in the course of this simulation. This was followed by a 25 ns MD simulation at a constant temperature of 298 K and an isotropic constant pressure of 10^3 MPa, throughout which the incoherent, "vaporous" system was condensed into a compressed "liquid". The system was again involved in a 5 ns MD simulation at a constant volume and temperature of 2673 K, upon which conformations of molecules in the dense "liquid of residues" varied in an accelerated manner to equilibrate the modelled system. This simulation was followed by equilibration in a 50 ns MD simulation at a constant temperature of 298 K and an isotropic constant pressure of 0.1 MPa, and then in a 50 ns MD simulation at a constant volume and constant temperature of 298 K. Finally, the potential energy of the obtained model of equilibrated "liquid of residues" was minimized by means of the L–BFGS[35] method. In the second stage, bonds between the termini of PVC_6 were gradually introduced into the prepared "liquid of residues". An adapted version of a previously developed iterative protocol for modelling epoxy resin crosslinking[32] was used. No more than 100 bonds between the termini of different PVC_6 chains, spaced from each other by no more than 0.7 nm, were introduced at each step of this process. After the introduction of new bonds between the terminal carbon atoms, potential energy optimization, MD simulation with a smooth increase of the force constant for new bonds, iterative optimization, and equilibration of the system by means of MD simulation at an anisotropic constant pressure with the 20 ns duration were performed. Thus, all 487 theoretically possible bonds connecting all short–chain PVC_6 fragments into a single looped macromolecule were introduced into the modelled system. As mentioned above, PVC S-7058M grade, whose number–average molecular weight ranged from 8×10^4 Da to 10^5 Da, was used to create the experimentally studied PVC composites. The molecular weight of the 2922–residue–long macrocyclic polymer molecule (PVC_{2922}) obtained by the iterative crosslinking process described above was 182619 Da. Dividing it into two equal linear polymer chains, we obtained two PVC_{1461} molecules that were closely packed in the simulation cell. The molecular weight of the PVC_{1461} polymer chain is 91309 Da, which lies in the middle of the molecular weight range characteristic of PVC S–7058M grade. In the third stage, the obtained simulation cell containing densely packed PVC and plasticizer molecules was subjected to deep equilibration. First, its potential energy was minimized using the flexible conjugate gradient method. The modelled system was then equilibrated using a 50 ns MD simulation at a constant temperature of 298 K and an anisotropic constant pressure of

https://doi.org/10.1007/s10118-026-3736-0

0.1 MPa with a compressibility of 10^{-4} MPa^{-1}. The system was then involved in a 20 ns MD simulation at a constant volume and temperature of 2073 K, which stimulated the polymer molecules to search for the best conformations. Further the potential energy of the system was minimized using the L–BFGS method, and 50 iterative equilibration steps were performed. The following operations were performed at each step of this process:

• A 2 ns MD simulation was performed at a constant temperature of 298 K and an anisotropic constant pressure of 0.1 MPa at a compressibility of 10^{-4} MPa^{-1}, in the course of which the dimensions of the simulation cell were relaxed.

• A 1 ns MD simulation was performed at a constant volume and temperature of 1273 K, throughout which the conformations of the polymer molecules were relaxed.

• Minimization of potential energy of modelled system using flexible conjugate gradient method. The obtained structure of the modelled system became the source state for the next step.

MD simulations at constant volume and high temperature, performed upon this equilibration procedure, were intended to speed up the varying of local conformations of polymer chains and plasticizer molecules, which were already packed into a dense phase. Because of this circumstance, their large-scale conformational movability is suppressed, so the general spatial packing of the polymer chains and plasticizer molecules can no longer change.

The potential energy of the structure obtained in the course of such iterative equilibration was further minimized using the L–BFGS method until the maximum force acting on the atom fell below 10^{-2} kJ/(mol·nm). The obtained state served as the initial state for a 100 ns equilibrium MD simulation at a constant volume and temperature of 298 K. The obtained trajectory was used for further analysis.

Modelling of Pure Plasticizers

The procedure of modelling of pure liquid plasticizers generally followed that for the "liquid of residues". First, 500 molecules of the modelled plasticizer were randomly distributed in a cubic cell with an edge of 18 nm, after which the potential energy of the constructed system was minimized. Then plasticizer molecules were uniformly distributed throughout the cell in the course of a 5 ns MD simulation at a constant volume and temperature of 2673 K. This was followed by a 15 ns MD simulation at a constant temperature of 298 K and an isotropic constant pressure of 10^3 MPa, throughout which the vaporous plasticizer condensed into a compressed liquid. The obtained simulation cell containing the compressed liquid plasticizer was involved in a 5 ns MD simulation at a constant volume and temperature of 2673 K. This was followed by equilibration in a 50 ns MD simulation at a constant temperature of 298 K and isotropic constant pressure of 0.1 MPa, and then in a 50 ns MD simulation at a constant volume and constant temperature of 298 K. The latter trajectory was used for further analysis.

Analysis of Equilibrium MD Trajectories

The analysis of equilibrium MD trajectories included the calculation of the root mean square deviation (RMSD) for PVC and plasticizer atoms heavier than hydrogen, clustering of trajectory frames by the conformation of PVC chains using the GROMOS[36] method, analysis of radial distribution functions, and the atom occurrence distribution $P(\boldsymbol{s})$ along the X, Y, and Z coordinates and in the XY, XZ, and YZ planes with the calculation of Shannon entropies H_s of the estimated distributions:

$$H_s = -\sum_i P(\boldsymbol{s}_i) \ln P(\boldsymbol{s}_i) \tag{1}$$

where the $\boldsymbol{s}$ vector is regarded as a one–dimensional coordinate X, Y, or Z, or a two-dimensional coordinate in the XY, XZ, or YZ plane; accordingly, $\boldsymbol{s}_i$ is nothing more than the coordinate of the center of the i^{th} bin used in the estimation of the distribution $P(\boldsymbol{s})$. Therewith, the decreases of entropy ΔH_s relative to the maximum entropy $H_{s,max}$ estimated for a given number of bins used in estimating the distribution were calculated. Suppose we used N bins for the X-direction and M bins for the Y-direction. The maximum entropy is achieved for the uniform distribution $P = N^{-1}$ in the one-dimensional case or $P = (MN)^{-1}$ in the two–dimensional case, and then,

$$\Delta H_X = H_{X,max} - H_X = \sum_i^N P(\boldsymbol{s}_i) \ln P(\boldsymbol{s}_i) + \ln N \tag{2}$$

$$\Delta H_{XY} = H_{XY,max} - H_{XY} = \\ = \sum_i^N \sum_j^M P(\boldsymbol{s}_{i,j}) \ln P(\boldsymbol{s}_{i,j}) + (\ln N + \ln M) \tag{3}$$

The value of the H_s entropy calculated in this way depends on the number of bins used to evaluate the corresponding distribution, and it varies for different modelled systems. Therefore, we calculated the normalized entropy h_s and its decrease Δh_s:

$$h_s = \frac{H_s}{H_{s,max}} \quad \Delta h_s = \frac{H_{s,max} - H_s}{H_{s,max}} = 1 - h_s \tag{4}$$

The analysis of equilibrium MD trajectories also included the calculation of radial distribution functions (RDF) for the carbon and oxygen atoms of the plasticizer relative to the carbon and chlorine atoms of PVC. The RDF and cumulative RDF were calculated with a 0.002 nm bin, and plasticizer atoms being distant no more than 2 nm away from the coordinating PVC atom were taken into account. The spatial distribution function (SDF) for the oxygen atoms of the plasticizer relative to the atoms of the PVC residues was calculated with 0.005 nm bin.

Upon the analysis, the topological characteristics of the polymer chains were assessed using the method described in Ref. [33]. Analysis was performed for the centroid of the most populated cluster, for which the potential energy was minimized. The spatial position of each polymer residue in the considered chain was described by the Cartesian coordinate of the carbon atom that was not bonded to a chlorine atom. Principal component analysis was performed for the coordinates of these residues of the analyzed chain, and the vector corresponding to the largest eigenvalue was taken as the principal spatial **L** axis of the polymer chain, along which it was mostly elongated. Further three geometric criteria were calculated for each residue.

• The s shift, being equal to the modulus of the residue r radius-vector projection on the **L** axis minus the shift of the starting residue of the chain, which is thus equal to zero.

• The r radius, being equal to the distance between the residue and **L** axis.

• The θ, being equal to the torsion angle between the normal from the residue to the **L** axis and the normal from the starting residue to **L**. Twist is calculated as an aperiodic value

that can vary from −∞ to +∞.

The possibility of halogen bond formation between the chlorine atoms of PVC and the oxygen atoms of the plasticizer molecules was assessed upon analysis of MD trajectories. A halogen bond between an X halogen atom covalently bonded to an R atom and a D atom donating electron density was considered to exist if the following conditions were simultaneously met[37]:

• The r_{XD} distance between the X and D atoms exceeded the sum of their van der Waals radii[38] by no more than 0.05 nm;

• The R–X–D angle θ_{RXD} was 180°±30°.

The free volume estimation was performed using the GROMACS "freevolume" tool, which probes the free volume with a rigid dummy of a given radius randomly thrown into the investigated space[39] The free volume fraction (ω_f) was estimated based on the van der Waals radii calculated by Bondi[38] while the probe radius was equal to zero. Fractional free volume f was estimated as follows[39]:

$$f = 1 - \frac{1.3V_{vdW}}{V_{cell}} = 1.3\omega_f - 0.3 \quad (5)$$

where V_{vdW} is a total volume of atoms calculated using van der Waals radii, and V_{cell} is a volume of simulation cell.

In addition, the glass transition temperature and volumetric coefficient of thermal expansion β were estimated using the same method as in the work[32], and the isothermal compressibility coefficient κ_T was estimated using the same method as in the work[40]. The corresponding dependencies of the simulation cell volume on temperature or volume were calculated using the Parrinello-Rahman[41] barostat with preliminary equilibration using a Berendsen barostat.

RESULTS AND DISCUSSION

Previous studies have described the synthesis and characterization of symmetrical dicarboxylic acid esters as PVC plasticizers[30,42,43]. In the present study, we constructed structural models of selected polymer compositions consisting of PVC plasticized with dicarboxylic acid esters (Table 1 and Fig. 2). Analysis of the structural organization of these compositions was carried out for frames of trajectories of equilibrium MD simulation with a duration of 300 ns, proceeded for each composite after the deep equilibration procedure described in the Methods.

Calculations of RMSD showed that the conformations of the PVC polymer chains stabilized after 20–30 ns of simulation for all compositions, indicating that the polymer chains had reached a state close to equilibrium. The conformation of the plasticizer molecules was also stabilized, but later (Fig. S1 in the electronic supplementary information, ESI). Analysis of the convergence of the average energy of electrostatic and van der Waals interactions between PVC and plasticizer with time (Figs. S6 and S7 in ESI) showed that this value converges after 50th ns of the trajectory. Thus, trajectory sections from 50 ns to 300 ns were involved in the further analysis. Clustering of the whole trajectory frames by the coordinates of heavy atoms of PVC molecules using the GROMOS method with a cutoff of 0.15 nm revealed that the conformations of the polymer molecules formed a dominant cluster, comprising between 29% and 45% of the frames. Thus, PVC molecules fitted into a stable conformation.

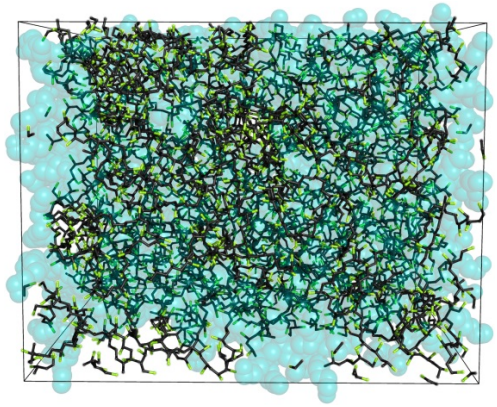

Fig. 2 Structural model of PVC composition **1**. PVC chains are shown by sticks, while plasticizer molecules are shown by transparent cyan surface. This image is intended for qualitative visualization; quantitative structural descriptors are presented in Tables S2–S4 (in ESI).

The distribution of atoms of the modelled system in the simulation cell volume was uniform for all modelled systems, both as a whole and in relation to PVC or plasticizer atoms. Neither one nor the other exhibited a pronounced concentration in certain regions of space, accompanied by the formation of individual phases and interphase boundaries. This observation is consistent with the experimental data obtained for samples of similar compositions.[31] In this work, dynamic mechanical analysis (DMA) showed that all composites exhibited a single peak in the mechanical loss tangent (tanδ) thermograms, which is direct evidence of the macroscopic single–phase nature of the studied PVC compositions and the absence of large-scale segregation of them. Nevertheless, some non-uniformity in the spatial distribution of plasticizer molecules was observed for **5**, **11** and **33** compositions (Fig. S4 in ESI). These observations were formalized through the calculation of Shannon entropies of distributions of atoms along the *X*, *Y*, and *Z* directions and in the *XY*, *XZ*, and *YZ* planes (Table S1 in ESI), and their decreases relative to ideally uniform distributions (Table S3 in ESI).

The non-uniformity of the plasticizer distribution revealed by the modelling enables to suggest the existence of regions with different local concentrations of components in the PVC compositions. Such non-uniformity may lead to a scatter in the local movability of polymer chains and affect the width of the relaxation peak of tanδ in the DMA thermograms. The experimental data demonstrate single tanδ peaks for all studied compositions, which testifies to the absence of macrophase segregation but does not exclude the influence of micro-heterogeneity on the shape of these peaks. A factor analysis of the tanδ peak parameters relative to the calculated characteristics of the PVC compositions was performed to test the hypothesis of microheterogeneity in the component distribution in the PVC composites. We considered the following parameters of the tanδ peak: the temperature T_{peak} at which tanδ reaches its maximum, the height of the tanδ peak M_{peak} measured from zero, and the width of the peak at half maximum measured from zero W_{peak} (Table S2 in ESI). The fol-

lowing relationships were found (Fig. S2 in ESI):

• The higher the average quantity of halogen bonds per trajectory frame, the higher T_{peak} temperature (R^2=0.65, p=0.096), which confirms the key role of directed electrostatic interactions in increasing the thermal stability of PVC compositions.

• The higher average energy of van der Waals interactions between molecules of pure plasticizer $\langle E_{VdW,Plast}\rangle$, the lower T_{peak} (R^2=0.76, p=0.053), said otherwise, the more intense dispersion interactions between molecules of pure liquid plasticizer, the higher the T_{peak} temperature.

• The greater the decrease in entropy Δh_{XZ}, the greater T_{peak} (R^2=0.65, p=0.1). In other words, the less uniformly the plasticizer is distributed in the simulation cell, the higher the T_{peak} temperature.

An increase in tanδ corresponds to the transition of the polymer composition from the glassy to the viscoelastic state, so that the maximum tanδ corresponds to the glass transition temperature. A markedly nonuniform distribution of the plasticizer within the polymer composite corresponds to the formation of domains with different local plasticizer concentrations. Each such domain should be characterized by its own glass transition temperature, which depends on the content of the components in the domain. Therefore, a markedly non-uniform composite, when heated, undergoes a continuous series of transitions lying within a certain temperature range instead of undergoing a single abrupt transition from the glassy to the viscoelastic state, which ismanifested by a broadening of the tanδ peak compared to the theoretically expected one. However, such domain formation and the resulting broadening of the tanδ peak is possible for polymer body of sufficiently large dimensions.

However, the characteristic size of the simulation cell in our study is a few nanometers, which should be smaller than the characteristic domain size; therefore, the tanδ peak broadening effect cannot be observed for the systems we modelled. Despite the observed small deviations in the plasticizer distribution from a perfectly uniform distribution, the structures of the polymer phases we modelled should still be considered as homogeneous solid solutions rather than dispersed systems. The observed variation in W_{peak} was associated with other factors. Nevertheless, MD modelling enables us to determine mutual relationships between the plasticizer efficiency, experimentally determined by DMA[31], and the structural features of the polymer phase at the atomic-molecular level.

The correlations between the emerging heterogeneity of the distribution of the plasticizer, described by the Δh_s entropy decrease, and the intensity of intermolecular interactions between the PVC polymer chains in the PVC compositions were also revealed:

• The greater value of the average energy of van der Waals interactions between polymer molecules in the PVC composition $\langle E_{VdW,\ PVC-PVC}\rangle$, the greater Δh_Y (R^2=0.77, p=0.052), said otherwise, the more intense dispersion interactions between PVC chains, the more deviation of plasticizer distribution along Y axis from uniformity.

• The greater value of the $\langle E_{VdW,\ PVC-PVC}\rangle$, the lower Δh_Z (R^2=0.88, p=0.02), said otherwise, the more intense dispersion interactions between PVC chains, the more uniformity of plasticizer distribution along Z axis.

• The greater value of the $\langle E_{VdW,\ PVC-PVC}\rangle$, the greater Δh_{XY} (R^2=0.85, p=0.025), the more intense dispersion interactions between PVC chains, the more deviation of plasticizer distribution in XY plane from uniformity.

• The greater value of the average energy of van der Waals interactions of plasticizer molecules in the liquid phase $\langle E_{VdW,Plast}\rangle$, the greater Δh_Y (R^2=0.75, p=0.059), id est, the more intense dispersion interactions between plasticizer molecules in the liquid phase, the more deviation of plasticizer distribution along Y axis from uniformity.

• The greater value of the $\langle E_{VdW,Plast}\rangle$, the lower Δh_{XZ} (R^2=0.85, p=0.026), that means, the more intense dispersion interactions between plasticizer molecules in the liquid phase, the more uniformity of plasticizer distribution in XZ plane.

Thus, the more intense the interactions between the PVC polymer molecules, the more heterogeneous the plasticizer distribution in the PVC composition. This is expected because the heterogeneity of the plasticizer distribution is the reverse side of the association of the polymer chains, which is expressed in their intense interactions. In addition, intense dispersion interactions between plasticizer molecules can promote their association in the PVC composition.

The densities of the modelled systems were approximately 1200 kg·m^{-3} and were slightly overestimated compared with the experimental measurements (Table 2). This overestimation of the calculated densities may stem from both the features of the force field and size of the simulated system. It was relatively small and contained only two polymer molecules of the same length. In contrast, the lengths of the polymer molecules in the real PVC composition are somewhat distributed. Therefore, the modelled systems were more ordered than real PVC compositions, which resulted in a slightly higher density. The simulation cells contained approxi-

Table 2 Calculated physico–chemical properties of modelled PVC compositions.

Composition	Density ρ (kg·m^{-3}) (calculated)	Density ρ (kg·m^{-3}) (experimental)	Fractional free volume f	Volumetric coefficient of thermal expansion β (10^{-6} K^{-1}) (glassy state)	Volumetric coefficient of thermal expansion β (10^{-6} K^{-1}) (viscoelastic state)	Glass transition temperature, (°C) (calculated)	Glass transition temperature, (°C) (experimental)	Coefficient of isothermal compressibility, κ_T, (TPa^{-1})
1	1249±4	1230	0.201	218±3	714±12	–55	–37	303±78
5	1244±6	1223	0.195	219±3	704±8	–60	–29	399±64
11	1222±6	1204	0.200	215±3	719±11	–61	–61	352±67
29	1234±5	1210	0.199	215±3	697±9	–61	–38	387±74
33	1238±5	1201	0.198	212±4	700±11	–60	–40	317±81

https://doi.org/10.1007/s10118-026-3736-0

mately 38% free volume, calculated using the Bondi[38] van der Waals radii. The free volume in the polymer phase determines the movability of the polymer chains, and its value directly affects the glass transition temperature. The high value of the calculated free volume, which is common to all studied systems, is consistent with their deep plasticization and a decrease in the glass transition temperature, correlating with the macroscopic properties measured experimentally.[31]

The calculated characteristics of the modelled systems (Table 2), such as the density and fraction of free volume, are consistent with the experimental data; the modelling also reproduces the relative trend of the glass transition temperatures. For example, the calculation correctly predicted that composition **11** had the lowest glass transition temperature in the series (–65 °C versus experimental –61 °C). This agreement confirms that the applied fragment condensation methodology enables constructing of adequate structural models reflecting the key features of plasticized PVC systems. Consequently, the correlations between the molecular parameters revealed in these models can serve as a reliable basis for interpreting experimentally observed macroscopic properties. In particular, the computationally obtained differences in the organization of the polymer matrix help explain the variations in the mechanical characteristics, such as the elastic modulus.

Thus, the highest elastic modulus E'=6700 MPa in the glassy state was measured for composition **5**[31]. Modelling shows that this system is characterized by a strong PVC-plasticizer interaction (Table 3) and a tendency toward an ordered helical conformation of the chains (Table 4). This can lead to a more "rigid" organization of the polymer matrix and, consequently, to a lower effective fraction of available free volume for relaxation processes, which is manifested in a higher modulus.

Analysis of the electrostatic and van der Waals interactions between the components of the modelled systems revealed some interesting relationships. It turned out that the experimentally measured onset temperature T_{start} increases with increasing energy of electrostatic interactions between PVC and plasticizer molecules, averaged over the frames of the equilibrium MD trajectory, $\langle E_{Coul,PVC-Plast} \rangle$. This dependence is approximated by a linear function with R^2=0.99 and p=4.1×10^{-4} (Fig. 3a):

$$T_{start} = (0.038 \pm 0.002) \langle E_{Coul,PVC\text{-}Plast} \rangle + (217 \pm 5) \quad (6)$$

The more intense the electrostatic interactions between PVC and the plasticizer, the lower the onset temperature, *i.e.* temperature, at which PVC composition begins to decompose.

On the other hand, modelling of pure plasticizers revealed that the experimentally measured T_{start} correlates with the energy of van der Waals interactions between plasticizer molecules, averaged over the frames of the equilibrium MD trajectory, $\langle E_{VdW,Plast} \rangle$. This dependence was approximated by a linear function with R^2=0.74 and p=6.1×10^{-2}:

$$T_{start} = (6.1 \pm 2.1) \times 10^{-4} \langle E_{VdW,Plast} \rangle + (69.5 \pm 21.4) \quad (7)$$

The more intense the dispersion interactions between the plasticizer molecules in the liquid phase, the lower the onset temperature.

In addition, the experimentally measured glass transition temperature T_g decreases with increasing energy of van der Waals interactions between plasticizer molecules in the PVC composition, averaged over the frames of the equilibrium MD trajectory, $\langle E_{VdW,Plast-Plast} \rangle$. This dependence was approximated by a linear function with R^2=0.78 and p=4.8×10^{-2} (Fig. 3b):

$$T_g = -(0.009 \pm 0.003) \langle E_{VdW,Plast\text{-}Plast} \rangle + (361 \pm 125) \quad (8)$$

The more intense the dispersion interactions between the plasticizer molecules in the PVC composition, the higher the glass transition temperature.

Table 3 Average quantity of halogen bonds in modelled PVC compositions per trajectory frame.

Bond type		Composition				
R–X	D	**1**	**5**	**11**	**29**	**33**
PVC/C_2–PVC/Cl	Plasticizer/O	55.1	56.1	45.5	46.5	42.5
PVC/C_2–PVC/Cl	Plasticizer/O_{ester}	21.2	20.4	16.1	16.3	13.8
PVC/C_2–PVC/Cl	Plasticizer/$O_{carbonyl}$	33.9	35.7	29.4	30.2	28.7

Table 4 Topological characteristics of polymer chains in modelled PVC compositions at the centroids of the most populated clusters: minimum and maximum shift s, radius r, twist θ.

Chain 1										
Composition	Min s	Max s	Min r	Max r	Min θ	Max θ	Turns –	Turns +	Wreath –	Wreath +
1	–275.88	30.20	0.63	100.25	–96.19	642.94	0.3	1.8	5467.7	818.0
5	–99.99	100.77	2.20	88.96	–14.02	448.11	0.0	1.2	37505.5	1173.7
11	–142.86	84.67	0.37	58.46	–267.06	798.77	0.7	2.2	1969.4	658.5
29	–0.28	263.92	0.40	73.68	–93.57	327.13	0.3	0.9	5621.0	1607.8
33	–192.93	9.83	0.34	109.80	–417.79	387.08	1.2	1.1	1258.9	1358.8
Chain 2										
Composition	Min s	Max s	Min r	Max r	Min θ	Max θ	Turns –	Turns +	Wreath –	Wreath +
1	–275.71	54.42	0.96	69.81	–615.17	69.10	1.7	0.2	855.0	7611.1
5	–1.36	201.98	3.29	90.67	–256.15	102.48	0.7	0.3	2053.3	5132.3
11	–190.28	54.04	0.60	100.20	–261.88	330.96	0.7	0.9	2008.4	1589.2
29	–229.05	29.10	0.40	92.53	–628.65	268.50	1.7	0.7	836.7	1958.9
33	–292.25	5.51	2.40	98.21	–231.14	158.83	0.6	0.4	2275.5	3311.5

https://doi.org/10.1007/s10118-026-3736-0

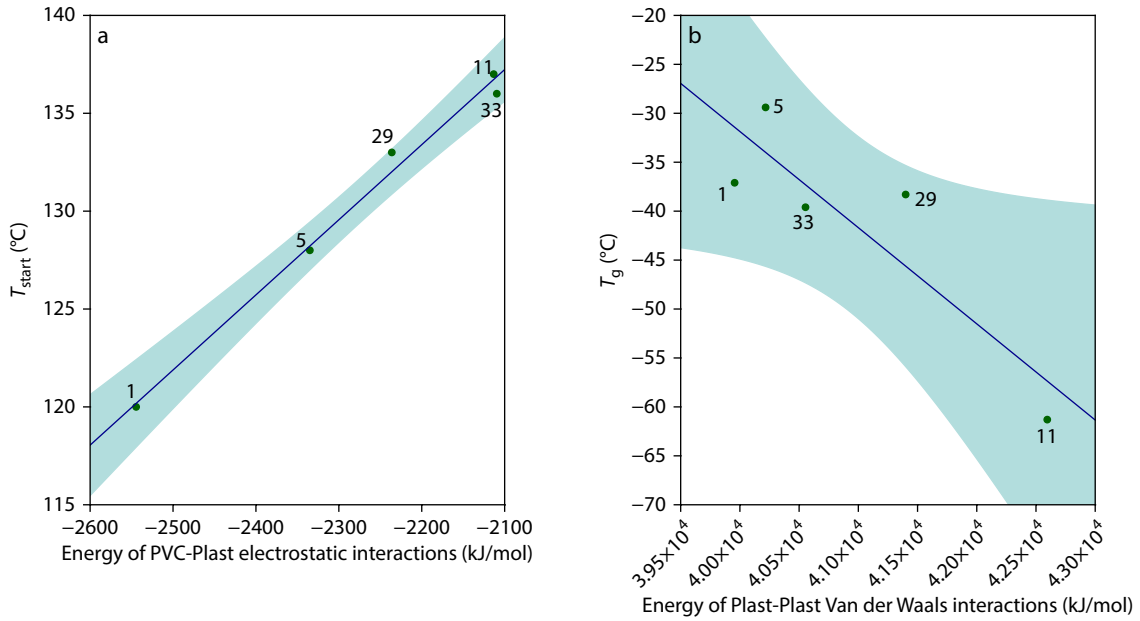

Fig. 3 (a) Dependence of the experimentally measured onset temperature T_{start} on the energy of electrostatic interactions between PVC and plasticizer molecules $\langle E_{Coul,PVC-Plast} \rangle$ according to the equilibrium MD simulation data. (b) Dependence of the experimentally measured glass transition temperature T_g on the energy of van der Waals interactions between plasticizer molecules $\langle E_{VdW,Plast-Plast} \rangle$ according to the equilibrium MD simulation data. A 95% confidence bands on the regression lines are shown by cyan.

We note that all the correlations presented here are based on only five plasticizer systems. With such a small sample size, even high R^2 values may be influenced by the natural co-variation of several molecular parameters (chain length, molecular size, and flexibility). Therefore, these relationships should be interpreted as preliminary trends rather than as statistically robust proofs of causality. The mechanistic interpretations derived from them are hypotheses that require validation on a larger and more diverse set of plasticizers.

The tendency of plasticizer molecules to associate or microsegregate limits their mobility and ability to uniformly "spread" PVC chains, which is necessary for effective plasticizing action. Thus, the thermal stability of PVC compositions is in a significant degree controlled by the strength of the specific (electrostatic) interaction between the plasticizer and PVC, and the efficacy of the glass transition temperature reduction is related to the ability of the plasticizer to minimize its association within the polymer matrix. Composition **11** serves as the most striking example, simultaneously demonstrating the highest thermal stability and the lowest glass transition temperature, indicating a successful balance between strong interactions with the matrix and a low tendency to associate. Our findings are in line with the structure-dependent plasticization efficiency reported by Li *et al.*[17,18] These authors demonstrated that alkyl chain length and branching significantly affect plasticizer compatibility and migration resistance in phthalate systems. Our simulations extend this knowledge to dicarboxylic acid esters and show a similar trend; increasing the acid chain length from C5 to C10 reduces the number of halogen bonds (Table 3) and alters the polymer chain topology (Table 4). These molecular-level changes correlate with the experimentally observed increase in low-temperature flexibility and decrease in thermal stability for longer-chain esters. Thus, our work directly links molecular descriptors to macroscopic properties, complementing previous simulation studies that have focused primarily on phthalates.

For the trajectories obtained from equilibrium MD simulations, a search for halogen bonds between PVC chlorine atoms and plasticizer oxygen atoms was performed using the geometric criteria described above. It should be noted that the molecular mechanical models we used did not explicitly model σ-holes on chlorine atoms by means of virtual sites, *etc*., so the presence of a halogen bond recognized between specific atoms suggests that its formation is possible due to other factors that folded the polymer and plasticizer molecules in the desired conformation. Because the force field does not account for σ-holes, these geometric contacts are not equivalent to energetic halogen bonds; they merely reflect the high probability of a close approach between Cl and O atoms. Therefore, the observed trends in contact counts were used only as a qualitative indicator of potential directionality and not as a quantitative measure of bond strength.

Nevertheless, on average, 42 to 56 halogen bonds were present at any given time in the modelled systems, whereby the majority of halogen bonds were formed by carbonyl oxygen atoms. Upon that, the quantity of halogen bonds. decreased as the chain length of the dicarboxylic acid residues increased (Table 3).

The calculation of the radial distribution functions (Fig. S5 in ESI) showed that the carbonyl oxygen atoms of the plasticizer were indeed more inclined to approach the chlorine atoms of PVC than the ester oxygen atoms. Upon that, the carbon atoms of the plasticizers were less inclined to approach the chlorine atoms of PVC than the oxygen atoms of

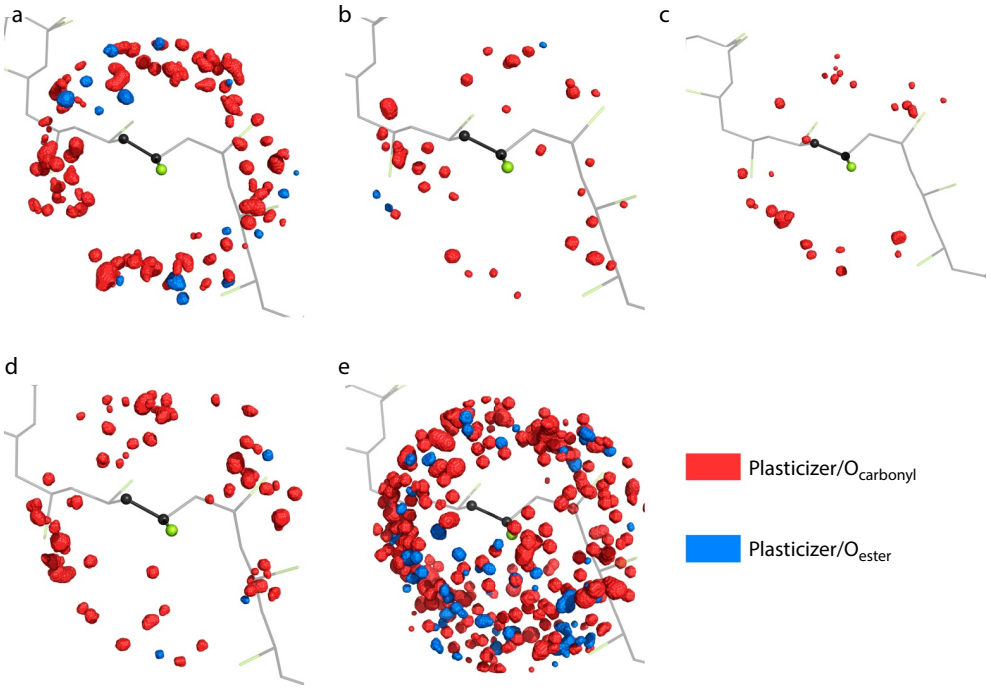

Fig. 4 Spatial distribution functions (SDF) for oxygen atoms of plasticizer relatively to PVC residue, shown by sticks and spheres. Dots show centers of voxels, at which probability is greater than 1.5×10^{-7}, and which are no more than 0.5 nm away from the chlorine atom of PVC residue. (a) Composition **1**, (b) composition **5**, (c) composition **11**, (d) composition **29**, (e) composition **33**.

both types. The calculation of the spatial distribution function (Fig. 4) confirms this observation, showing that the arrangement of the plasticizer oxygen atoms relative to the chlorine atom of the PVC residue is characterized by the most pronounced spatial selectivity in compositions **5** and **11** and the least in composition **33**. The greater ability of the carbonyl oxygen atoms to approach the PVC chlorine atoms can be explained by their greater steric accessibility compared to that of the ester oxygen atoms, access to which is hindered by the methylene groups of the ester substituents.

The decrease in the quantity of halogen bonds with carbonyl oxygen atoms ($O_{carbonyl}$) with the acid chain lengthens reflects a change in the mechanism of interaction between the plasticizer and PVC. An increase in the length of the flexible methylene chain between the carbonyl groups increases the conformational freedom of the molecule, reducing the probability of both carbonyl groups to be simultaneously optimally placed for interaction with chlorine atoms. Furthermore, the large nonpolar moiety "dilutes" the polar carbonyl centers, reducing their local concentration in the matrix. As a result, ester oxygen atoms (O_{ester}) become the main sites of specific binding, which relative contribution increases. At the same time, the role of nonspecific dispersion interactions between the aliphatic fragments of the plasticizer and PVC chains increased. This observed shift from directional carbonyl bonding to volume dispersion spreading is consistent with the macroscopic differences in the properties and suggests a gradual change in the dominant plasticization mechanism.

The proposed transition from carbonyl-dominated to dispersion-dominated plasticization is based on indirect evidence: the decrease in halogen bond counts with increasing acid chain length, the corresponding increase in van der Waals interactions between the plasticizer and PVC, and changes in the polymer chain topology (Table 4). Within the current data, the observed trends consistently indicate a gradual shift in the dominant plasticization mechanism.

This transition from directional carbonyl bonding to volume dispersion spreading explains the macroscopic differences in the properties. Thus, short–chain plasticizers (glutarate and adipate) are more strongly anchored in the polymer matrix *via* carbonyl groups, which favours good compatibility and resistance to migration. Long–chain plasticizers (sebacate) more effectively shield polymer chains owing to the flexible alkyl fragment, providing excellent low–temperature flexibility, which is consistent with the experimental data.[31] Thus, the change in the number of halogen bonds was confirmed by the change in the plasticization mechanism depending on the molecular structure.

Topological analysis of the polymer chain conformations revealed that both chains were twisted predominantly clockwise, whereby the first chain was twisted to the greatest extent in compositions **5** and **11** and the second chain in compositions **11** and **29**. Thus, the esters of adipic and azelaic acids favoured the helical twist of the PVC chain to a greater extent than the esters of glutaric or sebacic acids (Table 4). MD modelling indirectly confirmed the high conformational flexibility of the long methylene chain (C10) of the plasticizer through the topology of PVC chains. The topological characteristics varied widely for both PVC chains in the **33** system with dibutoxyethyl sebacate:

• The large scatter of the values between the minimum and maximum *s* shifts (for example, for chain 2) indicates that the polymer chains are strongly stretched along their main axis

https://doi.org/10.1007/s10118-026-3736-0

and occupy different positions.

• The large maximum radius *r* combined with the very small minimum *r* indicates that individual chain residues can deviate significantly from the axis or be very close to it, which is characteristic of chains with high local movability and the ability to adopt a variety of conformations (coils, loops, and elongated sections). This indirectly indicates a significant increase in the free volume and movability of the system, which is ensured by the flexible and long plasticizer.

• The wide range of θ twist confirms the ability of the chains to twist strongly, which is also a sign of high conformational freedom.

The optimal (average) length of the acid residue in adipate (C6) and azelate (C9) seems to maintain a balance between conformational flexibility, sufficient for accommodation to the helical geometry of the PVC chain, and structural rigidity or a specific directionality of interactions that promotes stabilization of the twisted conformation. Additionally, glutarate (C5) may be too short and rigid to effectively insert and stabilize the helix. Sebacate (C10) has excessive flexibility, and a bulky alkyl fragment, which effectively spreads the PVC chains, does not promote the formation of a stable helical conformation, but rather leads to a looser and more disordered placement of the polymer chains (which correlates with its superior low–temperature properties). Thus, the topological analysis data objectively confirmed that the structure of the plasticizer, in particular the length of the acid residue, significantly influences the conformation of PVC chains, with adipates and azelates being the most favourable to their helical twist.

Estimation of thermal expansion coefficients showed that in the glassy state, it is approximately 215×10^{-6} K^{-1}, and in the viscoelastic state, from 690×10^{-6} K^{-1} to 720×10^{-6} K^{-1}, while in the glassy state, these values are fairly close for all the studied compositions, and the thermal expansion coefficient in the viscoelastic state decreases with elongation of the dicarboxylic acid residue chain. The estimation of the glass transition temperatures taking into account the correction according to the Williams–Landel–Ferry equation underestimated the values by approximately 20 °C (Table 2). Despite the quantitative discrepancy, MD modelling correctly reproduces the relative trend; the calculation predicts the lowest T_g (–65 °C) for composition **11** (octyl butoxyethyl adipate), which is in qualitative agreement with the experimental minimum (–61 °C) for this set of samples.

It should be noted that achieving exact quantitative agreement between the simulated and experimental T_g values was not the primary goal of this work. The observed underestimation (about 20 °C) is within the typical range for MD simulations of glassy polymers using generic force fields such as GAFF, especially when combined with cooling rates many orders of magnitude higher than in the experiments. This systematic shift did not compromise the key findings because our conclusions are based on relative trends across the plasticizer series and mechanistic correlations (*e.g.*, halogen bond counts, interaction energies, and chain topology). The simulation correctly identified composition **11** as having the lowest T_g, which is in full agreement with the experiment. The absolute deviations for other compositions are non-uniform but do not alter the ranking or inferred structure–property relationships. Therefore, the model is considered suitable for comparative analysis and for elucidating the molecular mechanisms underlying experimental observations.

Our calculated trend in the glass transition temperatures (T_g) across the plasticizer series is consistent with the microscopic mechanism of local T_g reduction reported by Zhou and Milner[19], who showed that the effect of a plasticizer is spatially heterogeneous. Furthermore, the correlation we observe between electrostatic interaction energy and thermal stability aligns with the molecular design parameters identified by Li *et al.*[17,18], which emphasizes the importance of specific interactions between the plasticizer and PVC.

However, for compositions **1**, **5**, **29** and **33** the deviations between the calculated and experimental T_g values were larger, ranging from 18 °C to 31 °C (Table 2). These errors are nonuniform across the series, indicating that the models capture the underlying physics with varying accuracy. Several factors might have contributed to these discrepancies. First, the GAFF force field, which is generally reliable, may not fully describe specific interactions unique to PVC-plasticizer systems, particularly halogen bonds and the delicate balance between electrostatic and van der Waals terms. Second, the simulation cell size (a few nanometers) limits the long-range density correlations that influence glass transition in real materials. Third, the computational cooling rate is many orders of magnitude higher than that in the experiments, which can shift the simulated T_g unevenly, depending on the fragility of each composition. Finally, despite extensive equilibration, the slow relaxation modes of long polymer chains (especially in the presence of bulky or flexible plasticizers) may not be fully sampled. Acknowledging these limitations, the present models are best viewed as providing qualitative trends and semi-quantitative guidance, rather than exact predictions.

CONCLUSIONS

In the present work, we have obtained three-dimensional structural models of PVC compositions plasticized with dicarboxylic acid esters using molecular dynamics modelling methods and fragment condensation methodology. The estimation of the characteristics of the PVC compositions showed that their densities, fractional free volume, coefficients of thermal expansion, and glass transition temperatures were in qualitative and quantitative agreement with experimental data, confirming the adequacy of the models.

The simulations revealed correlations between the molecular structure of the esters and physicochemical characteristics of the PVC compositions. However, these correlations are based on a limited number of plasticizer systems (five) and on a specific MD/fragment-condensation framework; therefore, they should be considered as preliminary and model-dependent. We found that the number of halogen-bond-like contacts, the energy of intermolecular interactions between PVC chains and plasticizer molecules, and the degree of uniformity of the spatial distribution of plasticizer directly affect the temperature and width of the mechanical loss tangent peak, which reveals the nature of the relaxation behaviour of the material. Moreover, even in the absence of phase separation, the heterogeneity of the plasticizer distribution at the

nanoscale level, determined by its tendency to associate, significantly influences the width of the glass transition, indicating the importance of accounting for local concentration fluctuations upon designing the compositions.

Linear trends were observed between the onset decomposition temperature and the electrostatic interaction energy, as well as between T_g and the van der Waals energy of the plasticizer-plasticizer interactions. These trends, while model-dependent, offer potential semi-quantitative guidance for predicting thermal stability and plasticization efficiency, rather than direct criteria. A comparison of these relationships with the topological characteristics of polymer chain packing in space supports the hypothesis of a transition from the plasticization mechanism based on directed Cl···O contacts (characteristic for short-chain plasticizers) to the mechanism of bulk dispersion spacing of PVC chains (characteristic for long-chain plasticizers). This is consistent with such macroscopic differences as the increased thermal stability of adipates and the better low-temperature flexibility of sebacates.

It should be reiterated that these findings are derived from a specific MD/fragment-condensation framework and a limited set of five plasticizers; therefore, the quantitative trends and mechanistic hypotheses are model-dependent and require validation on broader datasets with alternative force fields.

Thus, the present work contributes to the fundamental understanding of the structural organization of plasticized polymer systems, once again demonstrating that the method of molecular dynamics modelling is a powerful tool for investigating the atomic-molecular structure of polymeric materials and their relationship with their physicochemical characteristics, harmoniously complementing the capabilities of traditional experimental methods for studying polymers. The preliminary relationships established here, pending validation on a broader set of compounds, may serve as a basis for guiding the targeted molecular design of plasticizers with the desired set of properties: high thermal stability, low glass transition temperature, optimal mechanical strength, and environmental safety. The developed methodology and identified descriptors pave the way for creating computational predictive models capable of significantly reducing the time and resources spent on the empirical selection of components for PVC compositions.

Conflict of Interests

The authors declare no interest conflict.

Electronic Supplementary Information

Electronic supplementary information (ESI) is available free of charge in the online version of this article at http://doi.org/10.1007/s10118-026-3736-0.

Data Availability Statement

The data that support the findings of this study are available from the corresponding author upon reasonable request. Correspondence and requests for materials should be addressed to G.I.M. (email:makarovgi@susu.ru).

ACKNOWLEDGMENTS

This research was financially supported by the Ministry of Science and Higher Education of the Russian Federation (No. FENU 2024–0005).

REFERENCES

1 Rahman, M., Brazel, C. The plasticizer market: an assessment of traditional plasticizers and research trends to meet new challenges. *Prog. Polym. Sci.* **2004**, *29*, 1223–1248.
2 Ali, M., Ueki, T., Hirai, T., Sato, T., Sato, T. Dielectric and electromechanical studies of plasticized poly(vinyl chloride) fabricated from plastisol. *Polym. Int.* **2013**, *62*, 501–506.
3 Titow, W.V. in *PVC Technology*, Springer, Dordrecht, **1984**, p. 59.
4 Wypych, G. in *PVC Formulary*, 3rd ed., ChemTec Publishing, Toronto, **2020**, p. 47.
5 Wang, M.Y., Zhou, N.Q., Hu, J. Effect of plasticizer (DOP) on cell structure and mechanical properties of extrusion-foamed PVC sheet. *Mater. Sci. Forum* **2015**, *815*, 601–606.
6 Tickner, J.A., Schettler, T., Guidotti, T., McCally, M., Rossi, M. Health risks posed by use of di-2-ethylhexyl phthalate (DEHP) in pvc medical devices: a critical review. *Am. J. Ind. Med.* **2001**, *39*, 100–111.
7 Gartili, A., Lapinte, V., Caillol, S., Briou, B., Jego, L. CNSL-based plasticizers, a promising and sustainable alternative to phthalates, a review. *RSC Sustain.* **2025**, *3*, 81–111.
8 Bocqúe, M., Voirin, C., Lapinte, V., Caillol, S., Robin, J. Petro-based and bio-based plasticizers: Chemical structures to plasticizing properties. *J. Polym. Sci. A Polym. Chem.* **2015**, *54*, 11–33.
9 Perito, E.D., Guerra, N.B., Giovanela, M., Machado, G., Silva Crespo, J. Chemical, thermal and mechanical evaluation of poly(vinyl chloride) plastisol with different plasticizers. *J. Elastomers Plast.* **2022**, *54*, 1277–1294.
10 Chen, Y., Zhou, S., Pan, S., Zhao, D., Wei, J., Zhao, M., Fan, H. Methods for determination of plasticizer migration from poly(vinyl chloride) synthetic materials: a mini review. *J. Leather Sci. Eng.* **2022**, *4*, 8.
11 Daniels, P.H. A brief overview of theories of PVC plasticization and methods used to evaluate PVC-plasticizer interaction. *J. Vinyl Addit. Technol.* **2009**, *15*, 219–223.
12 Misra, M., Mannodi-Kanakkithodi, A., Chung, T.C., Ramprasad, R., Kumar, S.K. Critical role of morphology on the dielectric constant of semicrystalline polyolefins. *J. Chem. Phys.* **2016**, *144*, 234905.
13 Ramos, J., Vega, J.F., Martínez-Salazar, J. A new insight into the conformation and melt dynamics of hydrogenated polybutadiene as revealed by computer simulations. *Soft Matter* **2016**, *12*, 3929–3936.
14 Mao, Y. F., Long, S. N., Li, Z., Tao, W. Q. Diffusion behavior of VOC molecules in poly(vinyl chloride) investigated by molecular dynamics simulation. *Int. J. Environ. Res. Public Health* **2023**, *20*, 3235.
15 Li, J., Jin, S. H., Lan, G. C., Xu, Z. S., Wang, L. T., Wang, N., Li, L. J. Research on the glass transition temperature and mechanical properties of poly(vinyl chloride)/dioctyl phthalate (PVC/DOP) blends by molecular dynamics simulations. *Chinese J. Polym. Sci.* **2019**, *37*, 834–840.
16 Lei, Q., Yi, X., Yu, W., Cheng, J., Ou, S., Xue, Q., Jiang, H. Molecular dynamics simulation of plasticizing effect of mixed dioctyl phthalate and isosorbide diheptanoate on poly(vinyl chloride) material. *Polymers* **2025**, *17*, 1655.

Graphical Abstract

Molecular Dynamics Investigation of the Mechanism of Poly(vinyl chloride) Plasticization by Dicarboxylic Acid Esters

Gennady I. Makarov, Irina N. Vikhareva, and Oleg I. Bol'shakov

South Ural State University, Russia; National Medical Research Centre of Cardiology named after Academician E.I. Chazov of the Ministry of Health of the Russian Federation, Russia

The structure of poly(vinyl chloride) (PVC) plasticized with dicarboxylic acid diesters (dibutoxyethyl glutarate, dibutoxyethyl adipate, octyl butoxyethyl adipate, dibutoxyethyl azelate, and dibutoxyethyl sebacate) was studied using molecular dynamics simulations. A transition from a plasticization mechanism associated with Cl···O interactions, which is characteristic of short-chain diesters, to a mechanism of volumetric dispersive distribution of PVC chains for long-chain esters was identified.

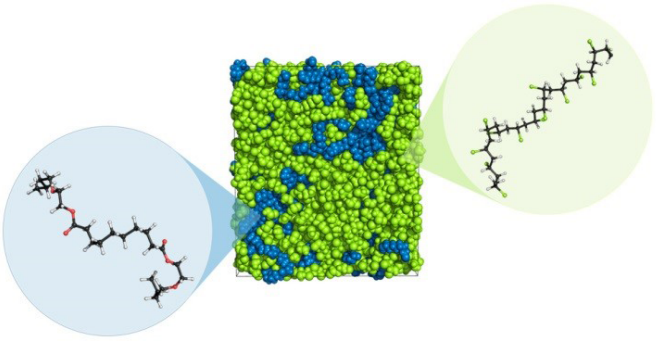

Chinese J. Polym. Sci., 2026 *https://doi.org/10.1007/s10118-026-3736-0*

17 Dongyang Li, D., Panchal, K., Mafi, R. Xi, L. An atomistic evaluation of the compatibility and plasticization efficacy of phthalates in poly(vinyl chloride). *Macromolecules* **2018**, *51*, 6997–7012.
18 Li, D., Panchal, K., Vasudevan, N.K., Mafi, R. Xi, L. Effects of molecular design parameters on plasticizer performance in poly(vinyl chloride): a comprehensive molecular simulation study. *Chem. Eng. Sci.* **2022**, *249*, 117334.
19 Zhou, Y., Milner, S.T. Average and Local Tg Shifts of Plasticized PVC from Simulations. *Macromolecules* **2018**, *51*, 3865–3873.
20 Wang, J., Wolf, R. M., Caldwell, J. W., Kollman, P. A., Case, D. A. Development and testing of a general amber force field. *J. Comput. Chem.* **2004**, *25*, 1157–1174.
21 Bayly, C.I., Cieplak, P., Cornell, W., Kollman, P.A. A well-behaved electrostatic potential based method using charge restraints for deriving atomic charges: the RESP model. *J. Phys. Chem.* **1993**, *97*, 10269–10280.
22 Neese, F. The ORCA program system. *Wiley Interdiscip. Rev. Comput. Mol. Sci.* **2012**, *2*, 73–78.
23 Neese, F. Software update: the ORCA program system, version 4.0. *Wiley Interdiscip. Rev. Comput. Mol. Sci.* **2018**, *8*, e1327.
24 Abraham, M.J., Murtola, T., Schulz, R., Pall, S., Smith, J.C., Hess, B., Lindahl, E. GROMACS: High performance molecular simulations through multi-level parallelism from laptops to supercomputers. *SoftwareX* **2015**, *1-2*, 19–25.
25 Bussi, G., Donadio, D., Parrinello, M. Canonical sampling through velocity rescaling. *J. Chem. Phys.* **2007**, *126*, 014107–014106.
26 Berendsen, H.J.C., Postma, J.P.M., Gunsteren, W.F., DiNola, A., Haak, J.R. Molecular dynamics with coupling to an external bath. *J. Chem. Phys.* **1984**, *81*, 3684–3690.
27 Hess, B., Bekker, H., Berendsen, H.J.C., Fraaije, J.G.E.M. LINCS: A linear constraint solver for molecular simulations. *J. Comput. Chem.* **1997**, *18*, 1463–1472.
28 Darden, T., York, D., Pedersen, L. Particle mesh Ewald: An Nlog(N) method for Ewald sums in large systems. *J. Chem. Phys.* **1993**, *98*, 10089–10092.
29 Wennberg, C.L., Murtola, T., Hess, B., Lindahl, E. Lennard–Jones lattice summation in bilayer simulations has critical effects on surface tension and lipid properties. *J. Chem. Theory Comput.* **2013**, *9*, 3527–3537.
30 Vikhareva, I.N., Manojlovíc, D. The effect of the structure of the alcohol component on the plasticizing ability of the ester of aliphatic dicarboxylic acid. *Appl. Sci.* **2024**, *14*, 10953.
31 Vikhareva, I.N., Kruchinina, P., Manojlovíc, D. The effect of dicarboxylic acid structure on the plasticizing ability of its ester. *Polymers* **2024**, *16*, 3372.
32 Makarov, G., Borodina, O., Makarova, T., Ignatova, A., Olivenko, N., Bartashevich, E., Sapozhnikov, S. Molecular dynamics study of cured ED-20 epoxy resin for predicting the glass transition temperature and relationship with structure features. *J. Phys. Chem. A* **2023**, *127*, 3894–3905.
33 Makarov, G. I., Deriabin, K. V., Islamova, R. M., Bartashevich, E. V. Structural organization of the self-healing copolymers of polydimethylsiloxane and Ni(II)pyridinedicarboxamide by the molecular dynamics and fragment condensation approach. *J. Inorg. Organomet. Polym. Mater.* **2025**, *35*, 5133–5143.
34 Notay, Y. Flexible conjugate gradients. *SIAM J. Sci. Comput.* **2001**,

22, 1444–1460.
35 Liu, D.C., Nocedal, J. On the limited memory BFGS method for large scale optimization. *Math. Program.* **1989**, *45*, 503–528.
36 Daura, X., Gademann, K., Jaun, B., Seebach, D., Gunsteren, W.F., Mark, A.E. Peptide folding: when simulation meets experiment. *Angew. Chem. Int. Ed.* **1999**, *38*, 236–240.
37 Desiraju, G.R., Shing Ho, P., Kloo, L., Legon, A.C., Marquardt, R., Metrangolo, P., Politzer, P., Resnati, G., Rissanen, K. Definition of the halogen bond (IUPAC recommendations 2013). *Pure Appl. Chem.* **2013**, *85*, 1711–1713.
38 Bondi, A. Van der Waals volumes and radii. *J. Phys. Chem.* **1964**, *68*, 441–451.
39 Lourenço, T.C., Coelho M.F.C., Ramalho, T.C., van der Spoel, D., Costa, L.T. Insights on the solubility of CO_2 in 1-ethyl-3-methylimidazolium bis(trifluoromethylsulfonyl)imide from the microscopic point of view. *Environ. Sci. Technol.* **2013**, *47*, 7421–7429.
40 Makarov, G.I. Molecular dynamics simulation of the electrical conductivity of α,ω-bis(3-aminopropyl) polydimethylsiloxane. *Mendeleev Commun.* **2025**, *35*, 1–4.
41 Parrinello, M., Rahman, A. Polymorphic transitions in single crystals: a new molecular dynamics method. *J. Appl. Phys.* **1981**, *52*, 7182–7190.
42 Vikhareva, I.N., Aminova, G.K., Mazitova, A.K. Ecotoxicity of the adipate plasticizers: influence of the structure of the alcohol substituent. *Molecules* **2021**, *26*, 4833.
43 Vikhareva, I. N.; Aminova, G. K.; Mazitova, A. K. Development of a highly efficient environmentally friendly plasticizer. *Polymers* **2022**, *14*, 1888.

https://doi.org/10.1007/s10118-026-3736-0